

Numerical investigation on effects of rotor control strategy and wind data on optimal wind turbine blade shape

Jin-Hak Yi^{*1,2}, Gil-Lim Yoon^{1,2a} and Ye Li^{***3}

¹Coastal Development and Ocean Energy Research Division, Korea Institute of Ocean Science and Technology, Gyeonggi 426-744, Republic of Korea

²Department of Convergence Study on the Ocean Science and Technology, Ocean Science and Technology School, Korea Maritime and Ocean University, Busan, Republic of Korea

³State Key Lab of Ocean Engineering, School of Naval Architecture, Ocean and Civil Engineering, Shanghai Jiao Tong University, Shanghai 200240, China

(Received June 11, 2012, Revised November 25, 2012, Accepted February 1, 2014)

Abstract. Recently, the horizontal axis rotor performance optimizer (HARP_Opt) tool was developed in the National Renewable Energy Laboratory, USA. This innovative tool is becoming more popular in the wind turbine industry and in the field of academic research. HARP_Opt was developed on the basis of two fundamental modules, namely, WT_Perf, a performance evaluator computer code using the blade element momentum theory; and a genetic algorithm module, which is used as an optimizer. A pattern search algorithm was more recently incorporated to enhance the optimization capability, especially the calculation time and consistency of the solutions. The blade optimization is an aspect that is highly dependent on experience and requires significant consideration on rotor control strategies, wind data, and generator type. In this study, the effects of rotor control strategies including fixed speed and fixed pitch, variable speed and fixed pitch, fixed speed and variable pitch, and variable speed and variable pitch algorithms on optimal blade shapes and rotor performance are investigated using optimized blade designs. The effects of environmental wind data and the objective functions used for optimization are also quantitatively evaluated using the HARP_Opt tool. Performance indices such as annual energy production, thrust, torque, and roof-flap moment forces are compared.

Keywords: blade element momentum theory (BEMT); pattern search; blade shape optimal design; parametric study; rotor control strategy; wind data

1. Introduction

Wind power is one of the fastest growing energy sources in the world. The wind energy industry is rapidly expanding in many countries in Europe, Asia, and the Americas. It is very important to use wind energy as an alternative energy source considering the need for energy security and reduction of carbon dioxide emission in view of the climate change issues (Vanem *et*

** Corresponding author for whole simulation framework, Professor, Email: ye.li.ocean@gmail.com

*Corresponding author for control strategy, Principal Research Scientist, Professor, E-mail: yijh@kiost.ac

^a Principal Research Scientist, Professor, Ph.D., Email: glyoon@kiost.ac

al. 2012). It is also necessary to develop the wind energy industry as a means of driving economic and industrial growth. In the United States, it has been reported that the wind energy industry will create 5 million new green jobs and supply 20% of the total energy demand by 2030 (US DOE, 2008). In Korea, there is a huge ongoing project to construct a 2.5 GW offshore wind farm in the west-south coastal area by 2019 (Lee *et al.* 2011). Considering the total national electricity generation capacity of about 70GW, the success of the project will significantly contribute to meeting electricity demands and also usher in a new era by breaking technical, environmental, and political barriers. Needless to say, it is well known that European countries are the most advanced in wind energy generation.

Wind turbines have been steadily getting larger to reduce the total cost of building a wind farm by the economics of scale. Many advances are being made regarding rotor blade design, geared and gearless technologies, generators, support structures such as foundations, monitoring, and wind farm simulation (Lee *et al.* 2010, Adhikari and Bhattacharya, 2011, Rebelo *et al.* 2012a, Rebelo *et al.* 2012b). For example, Sandia National Laboratory is presently developing a 13.2MW turbine blade with 100 m long for a publically available baseline rotor blade design (Griffith *et al.* 2012a, Griffith *et al.* 2012b). 6 MW class wind turbine blade with a 73.5 m long was successfully and commercially installed by Alstom in 2012. Gearless wind turbines are also becoming more popular owing to their lowcost and high-magnetic-density permanent magnet technology. Their elimination of a gearbox, which is the most frequently failing subsystem in wind turbines, also reduces the maintenance costs. Multibrid (multi-megawatt and hybrid) turbines, originated by Areva Multibrid GmbH, are also more widely adopted in the European offshore wind farm projects including *Alpha Ventus* project owing to its advantages such as small scale and compact drive system by combining conventional and direct-drive gearless drive-train systems. (deVries 2003). Wind turbine blade design is also a very important aspect of wind technology, which necessitates the development of related technologies.

During the process of wind turbine design, optimization is very critical for maximizing the power output and reducing the total cost. During optimization, it is very essential to evaluate the performance of the wind turbine blades, and the process can only be guaranteed by the use of reliable tools and techniques. There are two major frames of performance evaluation, namely, blade element momentum theory (BEMT) and computational fluid dynamics (CFD). The former can be used to evaluate the performance of turbine rotor blades in a steady state and with a simple design configuration, and it is fast and robust; the latter technique can also be used for unsteady 3-D and complex shaped blades, although it requires a lot of calculation time. It is therefore generally considered that BEMT is much more suitable for the design stage, and CFD is very effective for detailed analysis and final assessment.

The innovative horizontal axis rotor performance optimizer (HARP_Opt) tool was developed in the National Renewable Energy Laboratory (NREL) (Sale and Li 2010) and is becoming more popular in the wind turbine industry and in the field of academic research. This optimal design code uses BEMT for its core performance calculations and a genetic algorithm for optimization. Later, we successfully replaced the genetic algorithm with a pattern search. In this article, we summarize our effort regarding this work. After a brief presentation of the structure of Harp_Opt and other relevant background information, we discuss in detail the effects of the rotor control strategy, wind data, and an objective function on the turbine performance. More specifically, regarding the rotor control strategies, we discuss fixed speed and fixed pitch (FSFP), variable speed and fixed pitch (VSFP), fixed speed and variable pitch (FSVP), and variable speed and

variable pitch (VSVP). The discussed performance indices include power output, annual energy production, thrust, torque, and root-flap force.

2. Frameworks

2.1 HARP_Opt (Horizontal Axis Rotor Performance Optimizer)

HARP_Opt was originally developed by a group of researchers in the National Wind Technology Center and the National Renewable Energy Laboratory. It was developed for both wind and water applications. The currently available version uses a genetic algorithm for global optimization and for obtaining the Pareto solution in the case of multi objective optimization. The HARP_Opt code uses the WT_Perf (Wind Turbine Performance evaluation) code, which was also developed by NREL for evaluating the performance of wind turbine blades using the blade element momentum method (Buhl, 2009). HARP_Opt is therefore an integrated code that uses WT_Perf and generic algorithms (GAs) to optimize the horizontal axis wind and hydrokinetic turbines by artificial intelligence. HARP_Opt was recently used by Maki et al. (2012) to construct a meta model for multilevel wind turbine optimization, and many academic institutes have also adopted it for educational and research purposes (Fleming 2011).

2.2 Objective functions

HARP_Opt can handle the annual energy production (AEP) and the power coefficient (or power efficiency) as objective functions. To maximize the power coefficient, the total area (A_1) above the power curve in Fig. 1(a) between the cut-in wind speed (v_{cut-in}) and the rated wind speed (v_{rated}) can be used to construct an objective function as follows

$$\text{minimize } A_1 = \int_{v_{cut-in}}^{v_{rated}} (P_{rated} - P(v)) dv \quad (1)$$

where P_{rated} and $P(v)$ are the rated power and power output with respect to the wind speed v . By minimizing this area, the optimal blade shape can be obtained. The AEP can also be effectively used for a more economical and practical design if the probability density function (PDF) of the wind speed and direction at the installation site is available. The AEP-based objective function can be constructed as follows (see Fig. 1(b)):

$$\text{maximize } AEP = \int_{v_{cut-in}}^{v_{cut-out}} (P(v) p_w(v)) dv \times 8750 \quad (2)$$

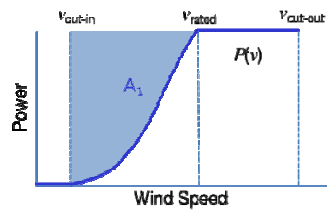
where $p_w(v)$ is the PDF of the wind data and the factor 8750 is used to convert the hourly energy production into annual energy production. $v_{cut-out}$ denotes the cut-out wind speed. The effects of the type of objective function on the optimization are investigated in detail in Section 4.5.

2.3 Rotor control strategies

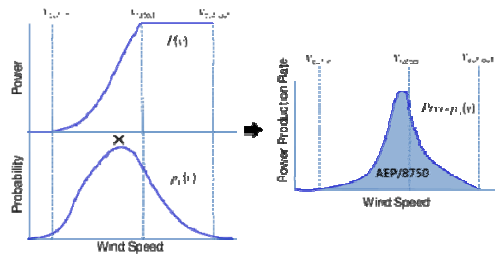
HARP_Opt can use several rotor control strategies to obtain maximum power coefficient and

power output, including (1) FSFP (passive stall regulation), (2) FSVP (active feather regulation), (3) VSFP(active stall regulation), and (4) VSVP(active feather regulation).

Fig. 2 shows the difference between the fixed speed and variable speed control strategies with regard to the optimized RPM schedule and power coefficient. As seen, the RPM (ω) is fixed to maximize the power coefficient near the mean wind speed for fixed-speed control, and it introduces the stall regulation for reducing the power output for wind speeds above the cut-out wind speed. Meanwhile, the RPM is proportionally increased to maintain the optimal power coefficient for variable-speed controls; i.e., the optimal tip-speed ratio (TSR), which is the most important parameter of a wind turbine rotor control strategy (Moriarty and Hansen 2005), can be maintained. However, it is noteworthy that the maximum power coefficient(ϵ) cannot exceed the Betz limit ($\epsilon_{BetzLimit} = 0.593$), as shown in Fig. 2(b). Moreover, the variable-speed control can be adopted when a synchronous-type generator is used, and AC-DC/DC-AC power controllers can be used to adjust the rotor speed by controlling the external torque; the fixed-speed control can be adopted when an induction-type generator is used. In the case of induction-type generators, the optimal rotational speed is limited to certain small ranges.

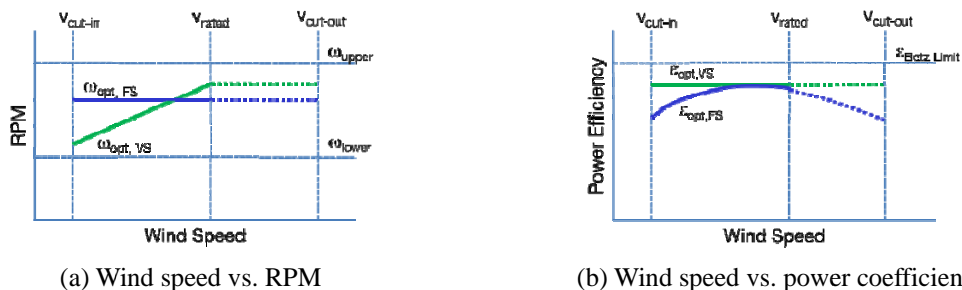


(a) Maximizing efficiency

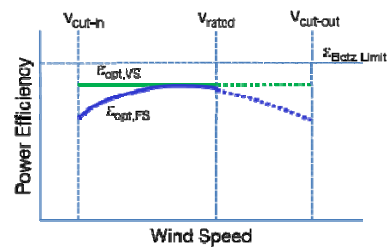


(b) Maximizing AEP

Fig. 1 Objective functions ofHARP_Opt



(a) Wind speed vs. RPM



(b) Wind speed vs. power coefficient

Fig. 2 Comparison of control strategies with regard to fixed speed and variable speed

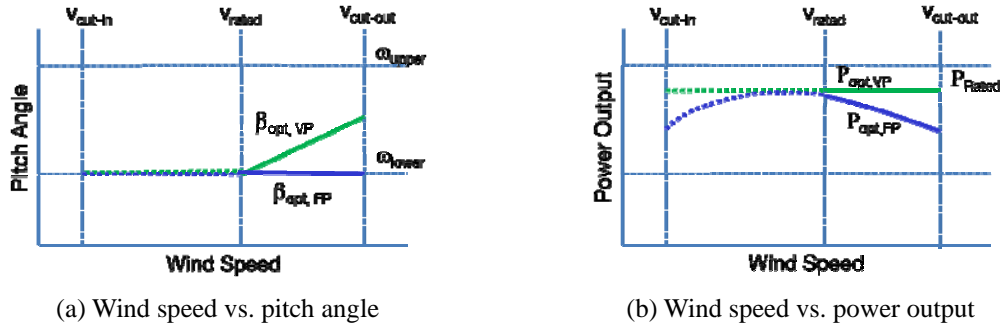


Fig. 3 Comparison of control strategies with regard to fixed speed and variable speed

Fig. 3 shows the differences between the fixed-pitch and variable-pitch control strategies in terms of the pitch angle schedule and power output. The pitch angle (β) can be adjusted to maintain the power output close to the rated power but not exceeding it. This is for protecting the generation facilities such as the gearbox, generator, and controller from excessive power generation above the facility capacity. In the case of the fixed-pitch control, the power output cannot be guaranteed to be the rated power output, as shown in Fig.3(b). It is, however, noteworthy that the power output of the fixed-pitch control can be maintained at the rated power by adjusting the rotor speed using variable-speed control.

3. Theoretical background

3.1 Blade element momentum theory and several correction methods

To evaluate the performance of wind turbine blades, HARP_OptusesWT_Perf, which is a modernized and enhanced BEMT code developed by NREL based on the PROP developed by Oregon State University. WT_Perf evaluates the performance of the turbine blade based on information on the blade shape and the aerodynamic characteristics, including the lift and drag forces of the particular type of airfoil (Buhl 2009). BEMT, originally attributed to Betz and Glauert (1935), assumes that (1) blades can be divided into small elements that act independently of surrounding elements and operate aerodynamically as two-dimensional airfoils (blade element theory), and (2) the loss of pressure or momentum in the rotor plane is caused by the work done by the airflow passing through the rotor plane on the blade element (momentum theory). In practice, BEMT is implemented by dividing the blades of a wind turbine into many elements along the blade span, from which the following equations are obtained

$$\tan \phi = \frac{U_{\infty}(1-a)}{\Omega r(1+a')} = \frac{1-a}{(1+a')\lambda_r} \quad (3)$$

where ϕ is the local inflow angle; U_{∞} and Ωr are the inflow velocity and tip speed, respectively; and λ_r is the TSR. From BEMT, the thrust (dT) and torque (dQ) distributed around an annulus

of width dr are respectively equivalent to

$$dT = B \frac{1}{2} \rho V_{total}^2 (C_l \cos \phi + C_d \sin \phi) c dr = 4\pi r \rho U_\infty^2 (1-a) a dr \tag{4}$$

$$dQ = B \frac{1}{2} \rho V_{total}^2 (C_l \sin \phi - C_d \cos \phi) c r dr = 4\pi r^3 \rho U_\infty \Omega (1-a) a' dr \tag{5}$$

Further information on BEMT, including enhancements, can be found in the references including Moriarty and Hansen (2005).

3.2 Pattern search method

The pattern search (PS) method is a type of “direct search” that uses only the function value and does not compute or approximate the gradient of the objective function. Therefore, PS can be successfully used for optimization even when there is a high level of discontinuities and nonlinearity in the feasible search space. The PS method was first introduced by Hooke and Jeeves in 1961 when they proposed the concept of “direct search” (Hooke and Jeeves 1961), and there has since been much research to enhance its performance and investigate its convergence characteristics. For example, the mesh size controlling technique was proposed by Fermi and Metropolis who used PS to determine the optimal fitting parameters of an experimental data set using Los Alamos Maniac (Lewis *et al.* 2000). Dolan *et al.* (Dolan *et al.* 2003) also investigated the convergence of the PS method using the positive basis method. Many studies have been carried out that combined engineering codes with PS to minimize engineering cost values (Alsumait *et al.* 2007, Wetter *et al.* 2003).

The PS is herein briefly introduced and more details are explained in Appendix. The basic operations consist of (1) Selection of the pattern vectors, (2) Polling, and (3) “Exploring move” with expansion and contraction. The pattern vectors, which represent the directions of the trial solution set, can be selected using the unit Cartesian vectors in R^n . The minimal and maximal pattern vectors are mostly used (see Fig. 4(a)). Thereafter, the polling operation, which is about deciding the next solution using the trial solution set, can be proceeded with. During the polling, the function values of the trial solution set are computed and compared with the function value of the current solution.

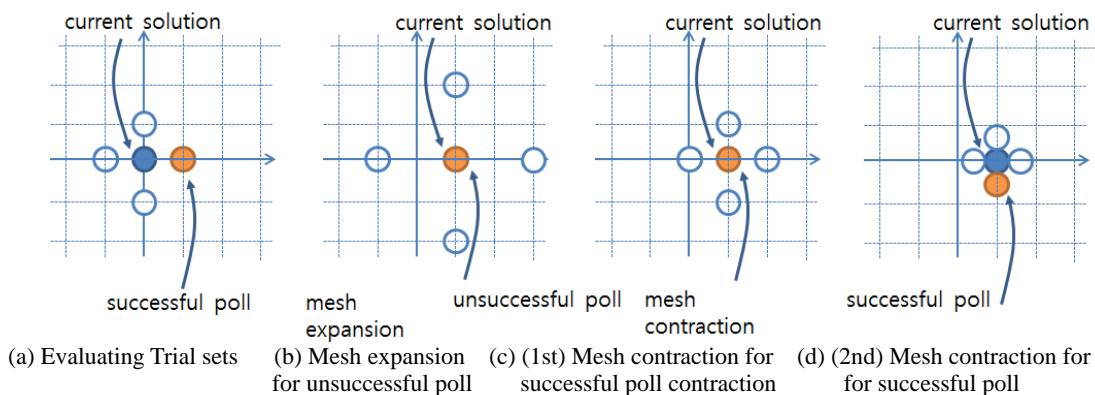


Fig. 4 Sample pattern search operation for two design variables

There are two types of poll operations: (1) Complete polling, which is when all the function values of all the solutions in the trial set are evaluated and compared, and (2) Incomplete polling, which is when only some solutions of the trial set have been compared and the process is terminated when a better solution is found. After polling, the exploring move and the next solution and trial set move with expansion and contraction. When the polling is successful, i.e., when there is a better solution in the trial solution sets (as shown in Figs. 4(a) and (b)), the mesh size can be increased. However, when the polling is unsuccessful, i.e. there is no better solution (as shown between Figs. 4(b) and (c) and between Figs, 4(c) and (d), the mesh size can be reduced. The primary procedure of PS is graphically summarized in Fig. 4.

4. SAMPLE analysis

4.1 Layout of sample study

In this study, the PS method was applied for optimizing the blade shape of the 1MW wind turbine. The basic layout of the sample wind turbine is shown in Table 1. A three-bladed horizontal-axis wind turbine with a rotor diameter of 50 m and hub diameter of 2 m was considered. FFA-W3-type airfoils were used. Regarding the wind condition, an operational wind speed in the range of 2-20 m/s was used; i.e., the cut-in and cut-out wind speeds (v_{cut-in} and $v_{cut-out}$) were 2 and 20 m/s, respectively. The probability distribution of the annual wind speed was assumed to be in accordance with the Rayleigh distribution, with a mean wind speed (v_{mean}) of 7.5m/s, as shown in Fig. 5. Regarding the rotor control strategy, the rotor speed and blade pitch angle were considered to be controlled by VSVP, with an operational rotor RPM range of 5-35 RPM. It should also be noted that, although a 1MW wind turbine was investigated in this study, larger turbines such as 5 and 7MW turbines can be evaluated by similar procedures, and the discussions of this study can be appropriately applied to them. It is also noticed that the rated wind speed (v_{rated}) is not given in Table 1 because the rated wind speed varies according to the blade design. If there is a target power coefficient ($C_{p,target}$), then the rated speed can be determined as follows,

$$v_{rated} = \left(\frac{P_{rated}}{C_{p,target} (0.5 \rho_{air} A_{swept})} \right)^{1/3} \quad (6)$$

where P_{rated} is the rated power output, and ρ_{air} and A_{swept} are the air density and swept area, respectively.

Table 1 Basic layout of the sample wind turbine

Parameters	Values	Parameters	Values
Number of blades	3	Rated power	1,000 kW (1 MW)
Rotor diameter	50 m	Airfoil shapes	FFA-W3-301, 241, 211
Hub diameter	2 m	RPM range for rotor	5-35 RPM
Operating wind speed	2-20 m/s	Wind distribution	Rayleigh dist. ($v_{mean} = 7.5\text{m/s}$)

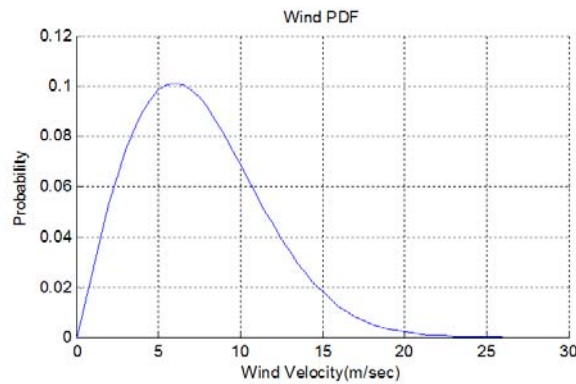


Fig. 5 PDF of wind data ($v_{mean} = 7.5$ m/s)

4.2 Optimization parameters

It is not practical to specify design variables such as the chord length and pretwisting angle at many points along the blade span due to the computational burden and the uniqueness problem. The number of design variables should therefore be reduced, which can be effectively done with the aid of Bezier curves using design variables at a limited number of control points (Sale and Li, 2010). In this study, 13 design variables were used; i.e., 10 design variables along the blade span for the chord length ($N_{chord\ length} = 5$) and pretwisting angle ($N_{pretwisting\ angle} = 5$), and three design variables for the percentage thickness ($N_{thickness} = 5$). For fixed-speed control strategies such as FSFP and FSVP, the optimal RPM value can also be optimized in the possible RPM ranges. The initial design values for the PS were specified as the mean values of the lower and upper bound values (LBVs and UBVs) shown in Table 2. It is noted that the initial values and lower and upper bounds can also be specified on the basis of experience. If the designer has some previous experiences or engineering insight in blade design, then the upper and lower bounds can be decided by the designer's engineering judgment, if not, the lower bounds can be specified not to be too small and structurally infeasible, and the upper bounds can be specified not to be too large. In this study, they were decided by considering the publically available blade shape and enough margins. The optimization parameters for the PS, such as the number of maximum iterations, are shown in Table 3.

Table 2 Control points and lower and upper bounds of chord length and pretwisting angles

Control point (m)		6.25	7.677	11.74	17.82	25
Chord length (m)	LBVs	0.5	0.1	0.1	0.1	0.1
	UBVs	1.5	1.5	1.0	1.0	0.25
Twisting angle (deg)	LBVs	-10	-10	-10	-10	-10
	UBVs	40	40	40	40	40

Table 3 Parameters for pattern search

PS parameters	Values		
Number of max. iterations	1000	Mesh size tolerance	1×10^{-6}
Pattern generation method	maximal, 2 N	Expansion factor	2.0
Polling method	Incomplete polling	Contraction factor	0.5

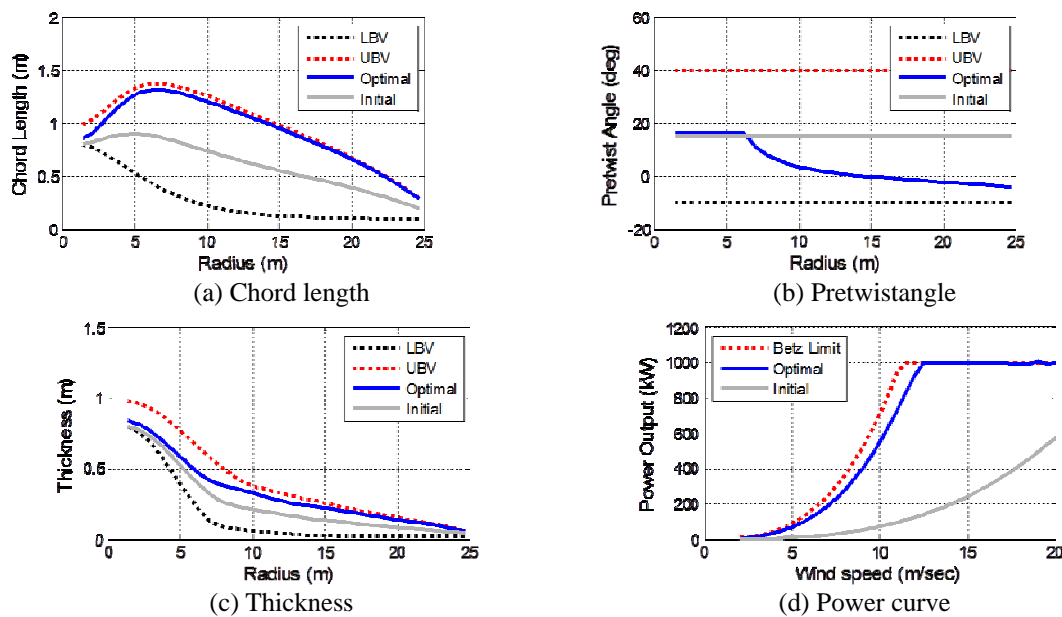


Fig. 6 Initial and optimal blade designs for VSVP control

Fig. 6 shows the in initial and optimized design curves of the chord length, pretwisting angle, and thickness along the blade span using the upper and lower bound curves. The curves were obtained using the Bezier curve and design values at the specific control points shown in Table 2. The power outputs for the initial and optimized blade shapes are also presented for the operating wind speed of 2-20 m/s. It is obvious that the power output for the initial design was much lower than that for the optimized design. The power coefficients were determined to be lower than 10% (c.f. Betz limit of 59.3%), and the AEP and capacity factor (CF) were respectively 499,574 kWh and 5.7% for the initial blade design. These values are also very low and unrealistic; although they are predictable considering that the blade shape was not optimized. For the optimized design, it was observed that the chord length somewhat converged to the upper bounds and that the pretwisting angle gradually decreased to as low as approximately 0°. The thickness also approached the upper bounds. These results indicate that the blade was a little bit bigger and thicker than the initial one.

It is also obvious that the power output was significantly enhanced by the optimization. The power coefficients between the cut-in and rated wind speed were determined to be about 46%, and the values of AEP and CF were also significantly enhanced to as much as 2,900,986 kWh and 33.1%,

respectively, which are almost six times those for the initial design. As mentioned earlier, these results were obtained for the conditions of VSVP control, a wind distribution with a mean value of 7.5 m/s, and an AEP-maximizing objective function. The effects of the rotor control strategies, wind data, and type of objective function on the optimal blade shape and the corresponding performance of the turbine blades were also thoroughly investigated. The summary of the results begin in the next section.

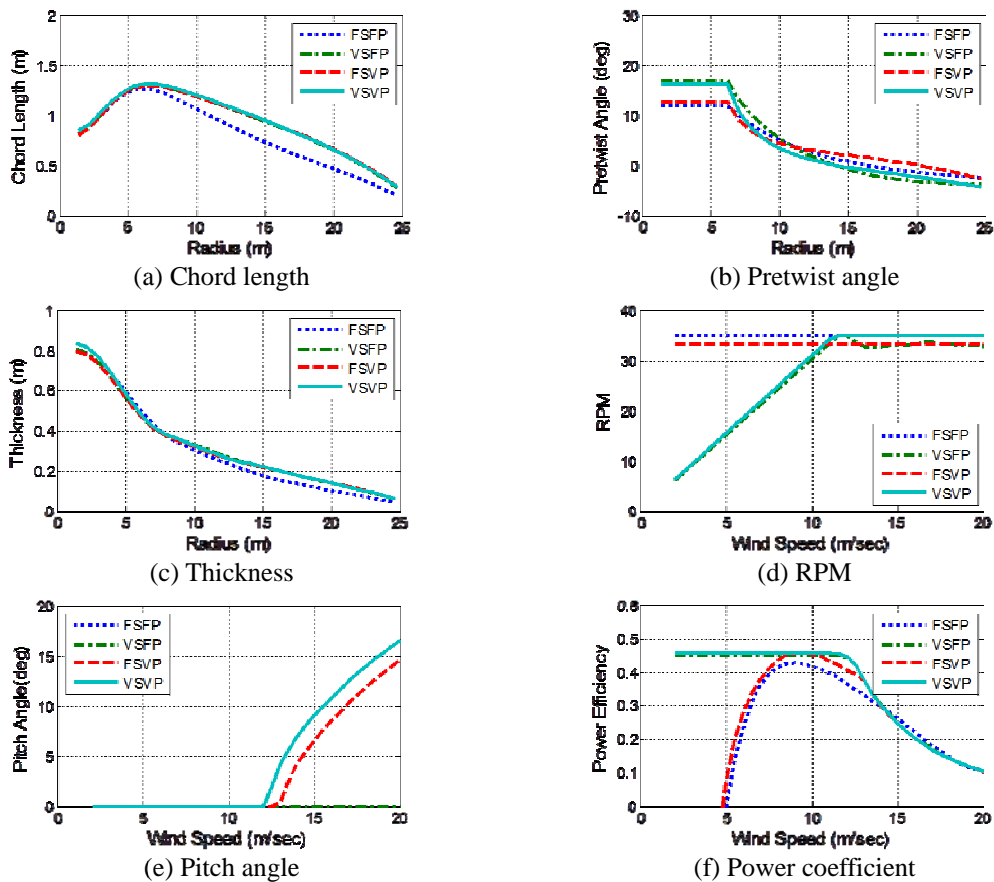


Fig. 7 Blade designs for different rotor control strategies

4.3 Effects of control strategy

Fig. 7 shows the optimized design shapes along the blade span and the optimal schedules of the rotor speed and pitch angle with respect to the wind speed for different rotor control strategies. From the results of the optimal chord length, it can be observed that the chord length for FSFP control is shorter than those for the others, and the results for the other three controls are similar. A similar trend can be observed for the thickness. The thickness for FSFP control is distinctively less than those for the other controls. This indicates that the optimal shape for FSFP control is somewhat

smaller; hence, it can be expected that the resulting thrust and torque forces may be lower than those for the other controls. It can also be observed that the optimal pretwisting angles for the fixed-speed controls, FSFP and FSVP, are smaller than those for the two variable-speed controls, VSFP and VSVP. Furthermore, it can be observed from the optimal schedule of the rotor speed in Fig. 7(d) that the RPM for FSFP was maintained at the upper RPM bound of 35 RPM, and that for FSVP was optimized as a little less. From the pitch angle schedule in Fig. 7(e), the pitch angle for VSVP was obviously controlled to reduce the resulting forces. When the power coefficient curves in Fig. 7(f) are considered, it can be easily understood that the power coefficient was maximized from the lower wind speed ranges around 2 m/s by adjusting the rotational speed; i.e., for the variable speed controls. For the fixed speed controls, the power coefficient was maximized near the mean wind speed (v_{mean}) in the range of 7.5-10 m/s.

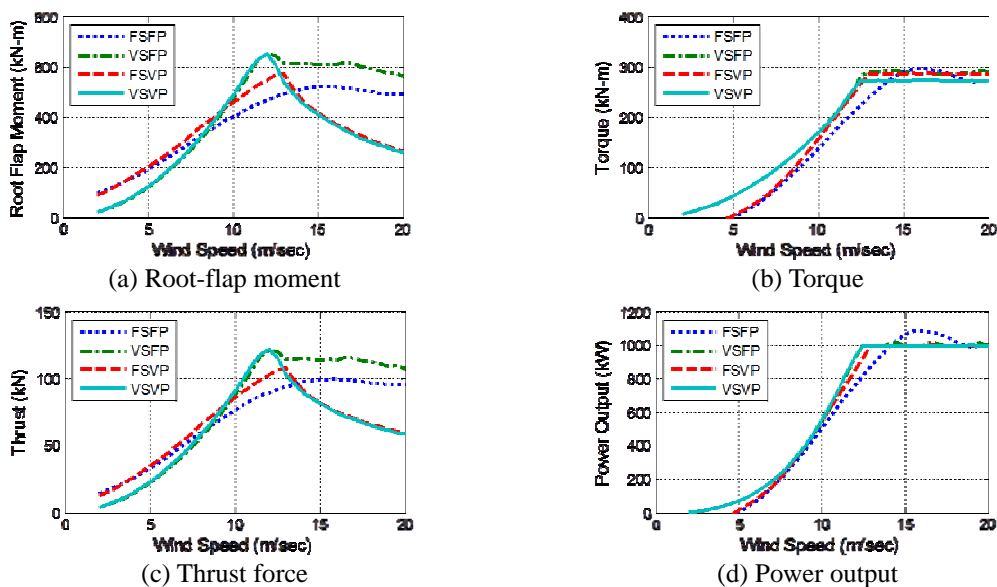


Fig. 8 Forces and power output of blade designs for different rotor control strategies

Fig. 8 compares the resulting forces, including the root-flap moment at the root of a blade, the torque of a main shaft, and the thrust of the aerodynamic forces using the power output curves with respect to the wind speed. It is obvious that these resulting forces were significantly affected by the applied control strategies. It can be observed that the forces between the cut-in and rated speeds gradually increased with the wind speed. Beyond the rated speed, the forces gradually decreased for the variable-pitch controls as shown in the Figs. 8(a)-(d). This means that the resulting forces could be effectively controlled by adjusting the pitch angle through a feather regulation. The root-flap moments and thrust force also gradually increased and maximized at the rated wind speed for the variable-speed controls, whereas the torque is not decreased to produce the rated power output with constant rotational speed of turbine blade. It was also observed that the resulting torque increased to produce a higher power output, whereas the root-flap moment and thrust were maintained as low as possible by means of the variable-speed control below the rated wind speed. Also, the root-flap moment and thrust were gradually reduced by an adjustment of the pitch angle for the variable-pitch

controls. In the event of an emergency or a normal shutoff to protect the wind turbine from an unexpected wind gust that exceeds the cut-out speed, it is very important to reduce the resulting forces to near the cut-out speed to prevent impact-like loading. In such a situation, a variable-pitch control can be of importance, especially in high wind conditions. From the curves in Fig. 8(d), it can be seen that the power output was not maintained at the rated level for FSFP control, which is not desirable for the integrity of generators. For the other controls, the power outputs were closely maintained near the rated level, with the power output curves for VSVP control being the best.

4.4 Effects of wind distribution

Fig. 9 shows three different PDFs of wind data that are in accordance with the Rayleigh distributions, with mean values of 6.5, 7.5 and 8.5 m/s. The overall shape is skewed to the right side and is somewhat widened when the mean value is increased. Using these three PDFs, the optimal turbine blade shapes were obtained and the resulting power output curves were compared with those of the control strategies in Fig. 10. The results showed that the power curve was not very sensitive to the wind data and the output curves were much more sensitive to the control strategies. When the following CV_{RMSD} (coefficient of variation of the root mean of squared deviation) index between two data set x and y was used as the relative difference index, the values of CV_{RMSD} are as shown in Fig. 11.

$$CV_{RMSD}(x, y) = \frac{RMSD(x, y)}{mean(x, y)} = \frac{\sqrt{\sum_{i=1}^N (x_i - y_i)^2 / N}}{\sum_{i=1}^N (x_i + y_i) / 2N} \quad (7)$$

It is noted that $RMSD_{6.5,7.5}$ in the legend of Fig. 11 represents the CV_{RMSD} between two power output curves for mean values of 6.5 and 7.5 m/s. The value of CV_{RMSD} for the FSFP control strategy is slightly greater than for the others, and is least for VSVP control. This means that the effect of the wind data on the power output for FSFP control is greater than for the others, with the power output for VSVP control being the most robust and least affected. However, when the results in Fig. 10 are considered, the differences for the different control strategies appear negligible from an engineering view point. This means that an optimized wind turbine blade for a certain wind farm site can be reasonably applied without additional modifications to other sites if the wind conditions are not significantly different. Hence, so-called standard blade designs for specific facility capacities are available.

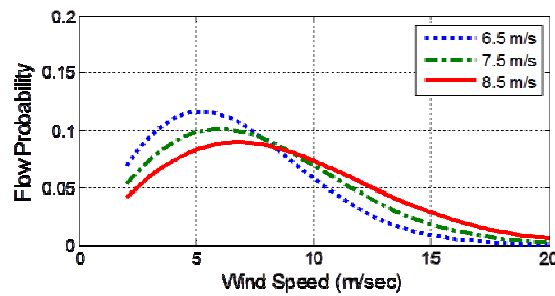


Fig. 9 PDF of wind data

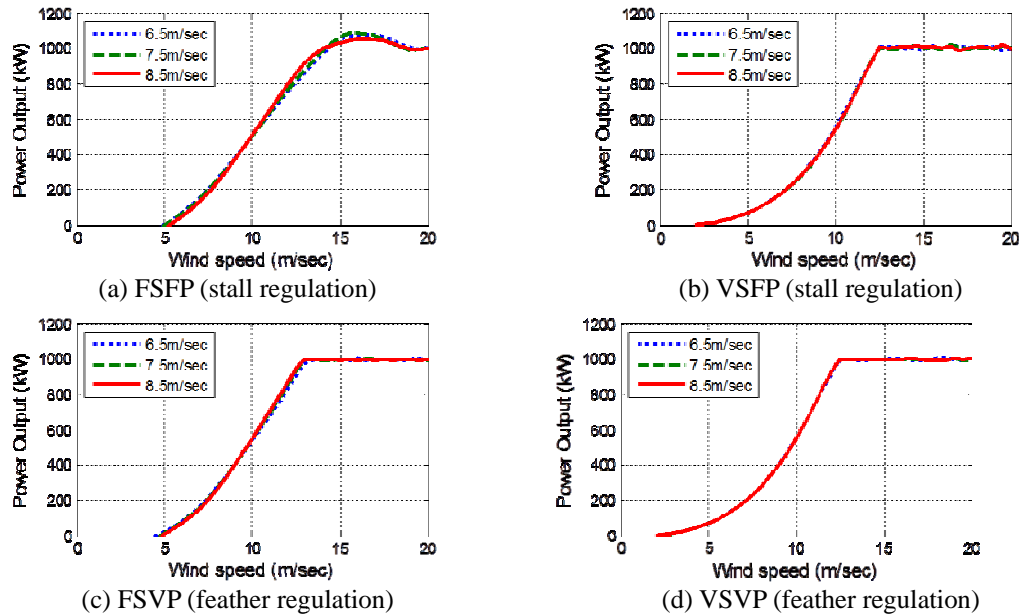


Fig. 10 Comparison of power curves for different control strategies and wind data

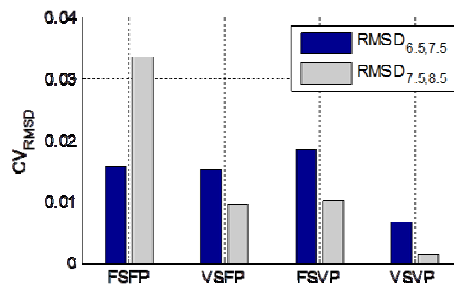


Fig. 11 Comparison of CV_{RMSD} of power output with respect to wind data for different control strategies

4.5 Effects of objective function

As mentioned earlier, two types of objective functions can be used to obtain the optimal blade shape, namely, the maximization of the power coefficient and the maximization of the annual energy production. Fig. 12 compares the results of the two types of objective functions. It is obvious that the results are not significantly different, except for FSFP control. This means that the optimal rotor blade design is affected by the type of objective function for FSFP control. The different values of CV_{RMSD} reflect the relative differences of the results more quantitatively, as shown in Fig. 13. The values for the fixed-speed controls are relatively higher than for the variable-speed controls.

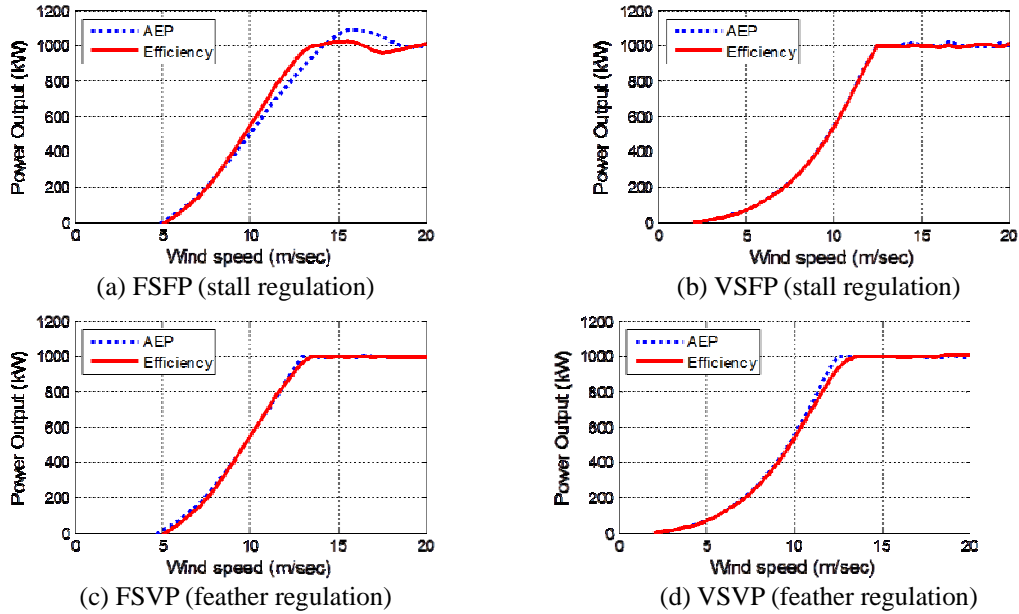


Fig. 12 Comparison of power curves for different control strategies and object functions

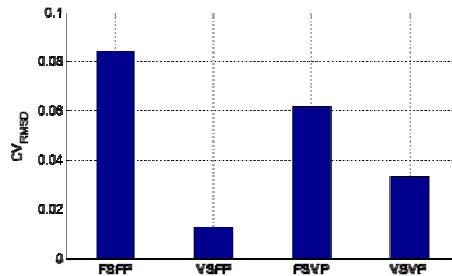


Fig. 13 Comparison of CVRMSD of power output for different objective functions

4.6 Summary

Table 4 summarizes the results of our parametric study on the effects of the control strategy, wind data, and type of objective function. In conclusion, the VSVP control was found to be the most promising in maximizing the AEP, as was also widely reported in various references including Li and Sales (2010). The capacity factor for a mean wind speed of 6.5 m/s was the least, whereas that for 8.5 m/s was the highest. Considering that the capacity factor is the ratio of the actual output of a power plant, such as the AEP, to the full rated capacity, it can be regarded as a measure of the economic benefit of power plants such as a wind turbine power plant. It is therefore required in deciding the rated power with regard to the wind data before the optimal design of the blade. The AEP values obtained from the optimization procedure for maximizing them were found to be slightly higher than those obtained for maximum coefficient. From the AEP view point, it was

observed that variable-speed controls were more beneficial for extracting the wind power than variable-pitch controls, whereas the pitch angle control was more beneficial for reducing the resulting forces near the cut-out wind speed, as described in Section 4.3.

Table 4 Summary of parametric study results

Objective function	Mean wind speed (m/s)	Control method	AEP (kWh/year)	Capacity Factor (%)
Maximizing AEP	6.5	FSFP	1,818,870	20.8
		FSVP	1,946,686	22.2
		VSFP	2,180,896	24.9
		VSVP	2,180,419	24.9
	7.5	FSFP	2,522,847	28.8
		FSVP	2,672,484	30.5
		VSFP	2,872,167	32.8
		VSVP	2,900,986	33.2
	8.5	FSFP	3,142,945	35.9
		FSVP	3,311,949	37.9
		VSFP	3,508,930	40.1
		VSVP	3,526,825	40.3
Maximizing coefficient	7.5	FSFP	2,616,457	29.9
		FSVP	2,611,634	29.8
		VSFP	2,854,287	32.6
		VSVP	2,817,021	32.2

5. Conclusions

A parametric study was carried out to investigate the effects of the rotor control strategy, wind data, and type of objective function on the optimal wind turbine blade shape and the power output. HARP_Opt was used for the optimization, with a modification in the optimization module; i.e., a pattern search method was used to reduce the calculation time and enhance consistency in the solutions. Four representative rotor control strategies including FSFP, VSFP, FSVP, and VSVP were investigated using a 1MW wind turbine. The following conclusions are made.

- VSVP control can be most efficiently used to obtain maximum power output by adjusting the rotor speed before the rated wind speed, whereas the resulting forces such as thrust and root-flap moments can be effectively reduced after the rated wind speed.
- FSFP control is not very reliable owing to the excessive power output, which means that stall regulation cannot be guaranteed, and the power output can significantly fall.
- The power output is not very sensitive to the wind condition, which means that the optimized wind turbine blade for a particular wind farm site can be reasonably applied to other sites without additional modifications.
- The power output is also not very sensitive to the type of objective function, although the maximization of the AEP is more adaptable than the maximization of power coefficient.
- Compared to variable-pitch controls, variable-speed controls are more effective for increasing

the power output at low wind speeds, whereas variable-pitch controls are more beneficial for reducing the resulting forces after the rated wind speed through the introduction of feather regulation.

Further parametric studies are necessary to investigate the effects of other factors such as the rated power output and initial design values. Further structural design and total cost optimization studies are also required for more practical designs.

Acknowledgements

This work was supported by the Korea Institute of Energy Technology Evaluation and Planning (KETEP) grant (20123030020110) and KIOST research program (PE98817). The authors would like to express their appreciation for the financial support.

References

- Adhikari, S. and Bhattacharya, S. (2011), "Vibrations of wind-turbines considering soil-structure interaction", *Wind Struct.*, **14**(2), 85-112.
- Alsumait, J.S., Sykulski, J.K. and Alothman, A.K. (2007), "Application of pattern search method to power system economic load dispatch", *Proceedings of the 3rd IASTED Asian Conference, Power and Energy System*, Phuket, Thailand, April 2-4.
- Buhl, M. (2009), NWTC Design Codes WT_Perf a Wind-Turbine Performance Predictor, <http://wind.nrel.gov/designcodes/simulators/wtperf/>.
- deVries, E. (2003), "Multibrid 5MW offshore wind turbine", *Renew. Energ.*, **6**(3).
- Dolan, E.D., Lewis, R.M. and Torczon, V. (2003), "On the local convergence of pattern search", *SIAM J. Optimiz.*, **14**(2), 567-583.
- Fleming, A. (2011), *Aquantis 2.5 MW ocean-current generation device-MHK*, Presentation from the 2011 Water Peer Review in which principal investigator discusses project progress to access Gulf Stream resource potential for marine and hydrokinetics devices.
- Glauert, H. (1935), *Division L: airplane propellers*, (Ed. Durand, W.F.), Aerodynamic Theory, Springer, Berlin.
- Griffith, D.T., Ashwill, T.D. and Resor, B.R. (2012), "Large offshore rotor development: design and analysis of the Sandia 100-meter wind turbine blade", *Proceedings of the 53rd AIAA Structures, Structural Dynamics, and Materials Conference*, Honolulu, HI, April 23-26.
- Griffith, D.T., Resor, B.R. and Ashwill, T.D. (2012), "Challenges and opportunities in large offshore rotor development: Sandia 100-meter blade research", *Proceedings of the AWEA WINDPOWER Scientific Track*, Atlanta, GA, June 3-6.
- Hooke, R. and Jeeves, T.A. (1961), "Direct Search Solution of numerical and statistical problems", *ACM J.*, **8**, 212-229.
- Lee, J.S., Kang, K.S., Park, B.M., Won, Y.J., Kim, B.G. and Ahn, N.S. (2011), "A study on current status and outlook of offshore wind development in Korea", *Wind Energy*, **2**(1), 6-14, in Korean.
- Lee, M., Lee, S.H., Hur, N., Choi, C.K. (2010), "A numerical simulation of flow field in a wind farm on complex terrain", *Wind Struct.*, **13**(4) 375-383
- Lewis, R.M., Torczon, V. and Trosset, M.W. (2000), *Direct search methods: then and now*, NASA/CR-2000-210125, ICASE Report No. 2000-26. NASA.
- Maki, K.J., Sbragio, R. and Nickolas, V. (2012), "System design of a wind turbine using a multi-level optimization approach", *Renew. Energ.*, **43**, 101-110.
- Moriarty, P.J. and Hansen, A.C. (2005), *AeroDyn Theory Manual*, NREL Technical Report,

- NREL/TP-500-36881.
- Rebelo, C., Veljkovic, M., Silva, L.S., Simoes, R. and Henriques, J. (2012), “Structural monitoring of a wind turbine steel tower - Part I: system description and calibration”, *Wind Struct.*, **15**(4), 285-299.
- Rebelo, C., Veljkovic, M., Matos, R., da Silva, L.S. (2012), “Structural monitoring of a wind turbine steel tower - Part II: monitoring results”, *Wind Struct.*, **15**(4) 301-311.
- Sale, D. and Li, Ye. (2010), “Preliminary results from a design methodology and optimization code for horizontal axis wind and hydro-kinetic turbines”, *Proceedings of the ASME 2010 29th International Conference on Ocean, Offshore, and Arctic Engineering, OMAE 2010*, Shanghai, China, June 6-11.
- US Department of Energy (2008), *20% Wind energy by 2030 - increasing wind energy's contribution to US electricity supply*, US Department of Energy, USA.
- Vanem, E., Natvig, B. and Huseby, A.B. (2012), “Modeling the effect of climate change on the wave climate of the world's oceans”, *Ocean Sci.*, **47**(2), 123-145.
- Wetter, M. and Wright, J. (2003), “Comparison of a generalized pattern search and a genetic algorithm optimization method”, *Proceedings of 8th International IBPSA Conference*, Eindhoven, Netherlands, August 11-14.
- Zhao, Z., Meza, J.C. and van Hove, M. (2006), “Using pattern search methods for surface structure determination of nano materials”, *J. Phys. Condensed Matter*, **18**, 8693-8706.

Appendix. Pattern search method for optimization

Consider the following optimization problem,

$$\text{Minimize } f(x) \quad (\text{A.1})$$

where $x \in R^n$, $f: R^n \rightarrow R$ and R^n denotes the n -dimensional real search space, i.e., the number of design variables is specified as n . And the basic operations of PS method consist of (1) selection of pattern vectors, (2) polling, and (3) “exploring move” with expansion and contraction as described in Section 3.2. Pattern vectors which represent the directions of the trial solution set, can be selected using the unit Cartesian vectors in R^n . Generally the minimal and maximal pattern vectors are utilized in most cases as follows (see Fig. A.1),

Minimal pattern vectors with $(n+1)$ unit vectors

$$D = \{e_1, e_2, \dots, e_n, -(e_1 + e_2 + \dots + e_n)\} \quad (\text{A.2})$$

Maximal pattern vectors with $2n$ unit vectors,

$$D = \{e_1, e_2, \dots, e_n, -e_1, -e_2, \dots, -e_n\} \quad (\text{A.3})$$

where e_i denotes the i -th unit Cartesian vector. Using the pattern vectors (d^i 's) and current solution (x_k), one can generate the trial solution set (x_k^i 's) with mesh size, Δm_k , as follows

$$x_k^i = x_k + \Delta m_k \times d^i \quad (\text{A.4})$$

where x_k and x_k^i denote the current solution and the i -th point in the trial solution set at k -th iteration step, respectively, and Δm_k denotes the mesh size and d^i is the i -th pattern vector in pattern vector set. Then, the polling operation, which represents how to decide the next solution using the trial solution set, can proceed. During polling, the function values for trial solution set are computed and compared with the function value of the current solution, and there are two types of poll operation available including complete polling and incomplete polling. After polling, the exploring move proceeds, and the next solution and trial set move with expansion and contraction. When the polling is successful, the mesh size will be increased as

$$\Delta m_{k+1} = 2 \times \Delta m_k \quad (\text{A.5})$$

If the polling is unsuccessful, then the mesh size can be reduced as

$$\Delta m_{i+1} = 0.5 \times \Delta m_i \quad (\text{A.6})$$

The expansion and contraction factors, 2 and 0.5, respectively, can be adjusted by the users, even though they usually used as 2 and 0.5 in many cases. The procedure for PS is summarized in Fig. 4 in Section 3.2 and Chart A.1.

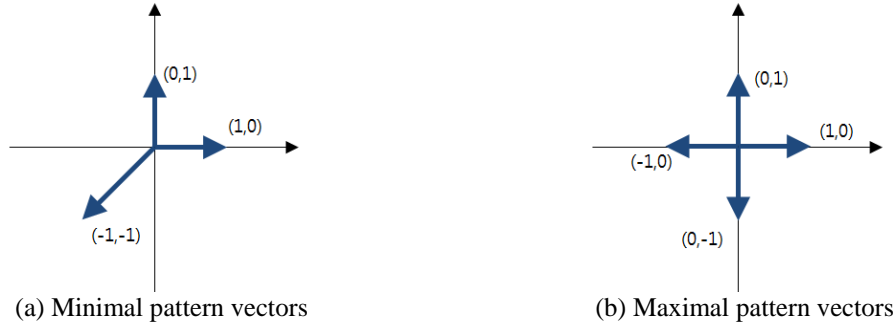


Fig. A.1 Minimal and maximal pattern vectors for the case with 2 design variables

Chart A.1 Procedure for Pattern Search Algorithm (Zhao *et al.* 2006)

- 1: Choose the set of pattern vectors, D ,
 - $2n$ vectors: $D = \{e_1, e_2, \dots, e_n, -e_1, -e_2, \dots, -e_n\}$
 - $n+1$ vectors: $D = \{e_1, e_2, \dots, e_n, -(e_1 + e_2 + \dots + e_n)\}$
- 2: Choose $\Delta m_0, x_0$ and Δm_{tol}
- 3: For $k = 1, 2, \dots$ Do
 - 4: if there exist $d^i \in D$ such that $f(x_k + \Delta m_k \times d^i) < f(x_k)$ then
 - 5: Set $x_{k+1} = x_k + \Delta m_k \times d_i$
 - 6: Set $\Delta m_{k+1} = 2 \times \Delta m_k$
 - 7: else
 - 8: Set $x_{k+1} = x_k$
 - 9: Set $\Delta m_{k+1} = 1/2 \times \Delta m_k$
 - 10: if $(\Delta m_{k+1} < \Delta m_{tol})$
 - 11: PS has converged and terminate.
 - 12: end if
 - 13: end if
 - 14: end for